Laser heat treatment of martensitic steel and dual-phase steel with high martensite content

Pierre Lapouge, Justin Dirrenberger*, Frédéric Coste, Matthieu Schneider

PIMM, Arts et Métiers-ParisTech, Cnam, CNRS, 151 bd de l'Hôpital, 75013, Paris, France

ARTICLE INFO

Keywords:
Laser heat treatment
Martensite
Dual phase steel
Softening
Processing

ABSTRACT

Laser heat treatment of galvanised steels with a martensite content superior to 80% were performed on a 1 cm wide area over an extensive temperature range [620 K - 1350 K]. The material softening induced is studied through uniaxial tensile testing and SEM microstructural observation. A treatment temperature close to Ac3 yields a massive increase in the ductility of the specimens while reducing the mechanical strength. This change in mechanical properties is associated with the nucleation of new austenite islands and the vanishing of the initial martensite laths. The results presented in this paper pave the way to localised variations of the strength-ductility trade-off, which could be useful for several industrial applications, particularly for enabling plastic forming or stamping of the martensitic steel sheets at low temperature.

1. Introduction

The desire to increase the fuel efficiency of cars has led the automotive industry to invest in projects aiming to reduce the weight of vehicles without compromising driver safety. Over the years, a major focus has been placed on the optimisation of the car body, commonly composed of heavy metallic parts, in order to minimise its mass [1,2]. For decades, steel manufacturers have regularly introduced new grades of advanced high-strength steels (AHSS) to meet these requirements and remain competitive against low-density alloys and composites [3]. Higher strength means that for the same load, less material and thus less weight are required to comply with component specifications. Hence, thinner structural components can be used without any loss of structural integrity.

AHSS mainly involve highly complex, thermomechanically processed steels. This label includes a wide range of grades from martensitic steels to steels with intricate microstructural morphologies such as transformation- and twinning-induced plasticity steels [4]. Martensitic and dual-phase steels, composed of martensite and ferrite phases, correspond to the very first generation of AHSS. The dual-phase structure combines the high strength of martensite with the good ductility of ferrite, thus yielding an adequate trade-off for sheet forming. As the martensite content increases, the strength of the material improves while the ductility decreases [5,6], which limits the industrial use of materials with a high martensite content for thin structures. An interesting compromise would be to soften the area where deformability is required while leaving the rest of the material untouched.

A laser heat treatment (LHT) is characterised by rapid heating and cooling rates with low interaction times between the material and the laser beam. At high temperature of treatment, the rapid cooling rate induces the quenching of the treated area and the hardening of the material. A strengthened surface can be interesting for example to increase the operating lifetime of a milling tool [7] or improve the crashworthiness of a part [8]. It has been extensively studied in the literature on a wide range of metals and alloys: titanium [9], copper [10], aluminium [11], or steel [12].

During the welding by laser of two parts, the difference in temperature between the weld zone and the parts generates a thermal gradient and the apparition of a heat affected zone (HAZ) in the vicinity of the weld. When joining two steels with a high martensite content, a soft zone is created in HAZ leading to a structural weak area [13,14]. This drop in strength is commonly attributed to a tempering of the martensite. On AHSS grade steel, the softening of the material is often seen as a limiting drawback for joining. However, tempering of martensite can also induce an increase in ductility [15–17]. Hence the local softening brought by LHT could grant an increase of ductility of martensitic steels where it's required.

Weisheit et al. [18,19] were among the firsts to report results on laser tempering of AHSS in order to improve the formability of the steel sheets. Their study mainly focused on treatments with peak temperatures below 800 °C. The dual phase and martensite steels showed a promising large increase in elongation and improvement in formability

* Corresponding author. Laboratoire PIMM, Arts et Métiers-ParisTech, Cnam, CNRS, 151 boulevard de l'Hôpital, 75013, Paris, France.

after laser treatment. Recently, Vogt et al. [20] also reported the effect on the softening of a manganese-boron steel, of the duration of exposure to the laser with a studied range between 50 and 3600 ms. They demonstrated that a long interaction lead to a more significant softening of steel with a treatment more uniform through the thickness of the sheet.

There is still a lack of experimental data to accurately determine the resulting softening after LHT as a function of temperature reached during the process. Most authors assumed that the optimum is in the region of conventional tempering below the austenitisation temperature based on results obtained on weld samples and the soft area in HAZ [21,22]. Capello and Previtali [23] did compare LHT with a tempering treatment at 600 °C and a "annealing" treatment at 900 °C. If the tempering treatment gave the most softening, the range of temperatures remain wide between the two studied temperatures.

The present paper aims to extensively characterise the effects of LHT temperature on martensitic steel and dual-phase steel with a high martensite content. The study was conducted over the entire range of temperatures (620 K - 1350 K) with uniaxial tensile tests used to characterise the mechanical behaviour and electron microscopy used to observe the microstructural changes after each treatment. A large laser spot and thin sheets were used to ensure that the heat treatment was as uniform as possible on the tensile specimens. This feature allows to accurately determine the strength and ductility of the laser treated specimen at a given temperature.

2. Experimental setup

The two high-strength steels used in this study are commercialised by ArcelorMittal as DP1180EZ and MS1500EZ. The DP1180 grade is a dual-phase steel comprising more than 80% martensitic phase and the remainder of ferritic phase, while the MS1500 is a fully martensitic grade. The steels were used in their as-received state, *i.e.* cold rolled into 1-mm thick sheets and galvanised with a thin zinc layer of a few microns to resist corrosion. The upper limits of the steel compositions are provided in Table 1.

The laser treatments were carried out with a 10 kW Trumpf continuous laser source on large rectangular samples measuring 12 × 20 cm in both the rolling (RD) and transverse (TD) directions. The laser spot is a 1.2 × 1.2 cm^2 square with uniform energy density. The samples were mounted on a linear actuator moving at a constant speed of 10 mm. s^{-1}. The experimental setup is represented in Fig. 1. The samples were irradiated at a constant power ranging from 300 W to 1650 W in order to scan a large spectrum of temperatures ranging from room temperature to well above the austenitisation temperature of low-carbon steels. Fourteen different powers corresponding to fourteen different peak temperatures were tested for both materials. Three specimens were used in each condition to characterise their mechanical behaviour using uniaxial tensile tests and microstructural observations.

The temperature reached in each condition is measured every millisecond with several thermocouples of type K welded to the backside of the samples. The temperature on the irradiated side is not directly measured but instead computed using the software COMSOL Multiphysics (see Section III.1 below). Neither compressed air nor neutral gas flows are used during the experiments. A single pass is performed for each laser treatment without any overlapping.

The simulations involve a simple finite-element model of a localised heat source on a homogenous piece of metal. The aim of the simulation is not to accurately reproduce the experimental process but rather assess the thermal distribution profile in the sample at the peak temperature. In particular, the physical changes and influence of the coating are not directly considered in the model, and the thermal losses by radiation or exchange with the atmosphere are disregarded.

Tensile specimens were laser-cut in sheets centred on the laser tracks. The specimens had a reduced section with a 6 mm width and 35 mm length. This small width compared to the laser spot allows good treatment uniformity to be achieved on the specimen surface. All the specimens were tested at room temperature under a strain rate of 10^{-3} s^{-1} in a uniaxial tensile test machine using an electromechanical extensometer.

Microstructural characterisations were conducted on the cross-section before and after laser treatment using scanning electron microscopy (SEM). Prior to the observations, the samples were prepared by grinding with silicon carbide abrasive sheets with grit sizes of 600, 1000, 1200, and 2000, followed by cloth polishing using 9, 3, and 0.25 µm diamond suspension solutions. Energy dispersive X-ray spectrometry (EDS) measurements were carried out on the cross-section of the treated steel sheets along lines to quantify the changes in the zinc coating after treatment. The samples were then etched in a 3% nital solution for a few seconds to enhance the contrast between ferrite and martensite in the SEM.

Table 1
Typical composition of the DP1180EZ and MS1500EZ grades.

	C_{max}(wt%)	Mn_{max}(wt%)	Si_{max}(wt%)
DP1180	0.15	1.8	0.2
MS1500	0.23	1.8	0.25

3. Results

3.1. Thermal evolution modelling

Fig. 2 depicts the average values of maximum temperatures measured with thermocouples on the samples for each condition. A measurement was only considered valid if the thermocouple was well centred on the laser track and if the temperature curve matched the expected shape, i.e., an asymmetrical bell shape as seen in Fig. 3. This shape can be explained by the differences between the heating and cooling rates. With our choice of parameters for the laser spot, the heating rate is several time higher than the cooling rate on the centre of the laser track. Because of the temperatures reached, the zinc coating became liquid and even evaporated at the highest applied powers. Despite the changes undergone by the coating, it is worth noting that the thermocouples always remained attached to the steel sheets after treatment.

As shown in Fig. 2 and described in the rest of this article, the critical temperatures of the phase transformation of austenisation (Ac1 and Ac3) and the start temperature of the transformation of martensite (Ms) are calculated based on a 0.2% carbon steel using the empirical formula of Andrews [24]. The indicative values (Ms = 730 K, Ac1 = 1000 K, and Ac3 = 1100 K) may differ from the actual values by a few tens of Kelvin degrees depending on the exact steel composition.

The temperature differences between DP1180EZ and MS1500EZ can be explained by a discrepancy between the absorptivities of the two zinc coatings, as MS1500EZ sheets appeared to be slightly more reflective than DP1180EZ.

The temperature during treatment is modelled with the same set of parameters for both materials, with the exception of the absorptivity used to fit the numerical values on the experiments. Table 2 lists these parameters. Constant conductivity (λ), specific heat capacity (Cp), and density (ρ) gave satisfying results over the complete range of temperatures with a corrected absorptivity for each treatment. For MS1500EZ, the coefficient of absorption (α) decreased progressively from 0.57 to 0.345 as the power increased (up to 1500 W), while for DP1180EZ it decreased from 0.61 to 0.41 (up to 1300 W). The highest power, 1380 W for DP1180EZ and 1650 W for MS1500 EZ, is not modelled. At this power, the zinc coating is completely removed (see Section II.3 below), which leads to a massive change in the absorption coefficient. This explains the offset of measurements for the last points in Fig. 2 compared to the linear behaviours observed for the other

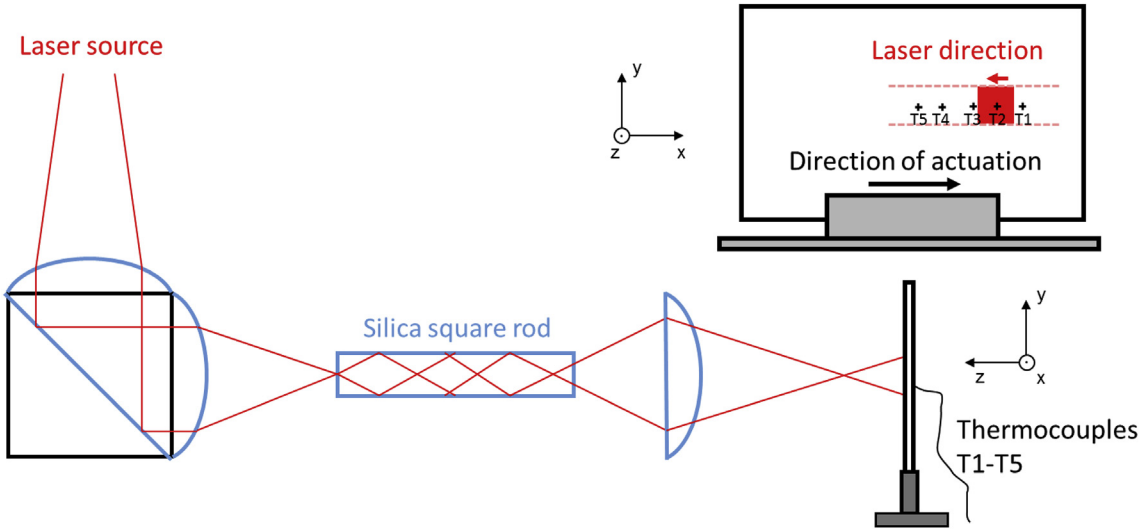

Fig. 1. Experimental setup, with five temperature measurements being performed in each condition.

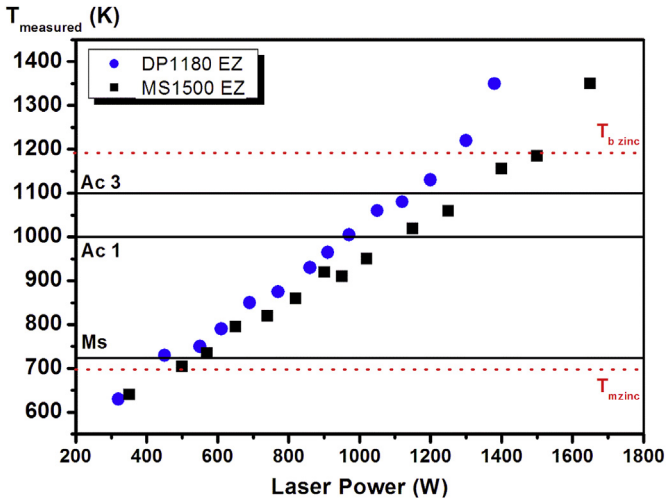

Fig. 2. Temperatures measured by thermocouples for each applied laser power.

measurements with the applied power.

Fig. 3a shows the temperature changes of a point on the backside of the samples at the centre of the laser track that were measured with a thermocouple as well as the corresponding simulation. As a first approximation, the model adequately reproduces the temperature changes during laser treatment. The hypothesis of constant coefficients during the entire treatment is obviously false, as the temperature increase seen in the experimental data is not as linear as in the numerical simulations during the heating phase (Fig. 3a).

All experimental conditions were modelled, as shown in Fig. 3b for DP1180EZ. The difference between the highest temperature on the irradiated surface and the highest temperature on the backside does not exceed 50 K (3.6% of the highest temperature point) at 1300 W. The difference is even lower at a low power, being 10 K at 320 W (2.6% of the highest temperature point).

The irradiated area cools down rapidly. In the first ms, the top surface cools down at several hundred K/s, while the treated area cools down at rate of several tens of K/s.

3.2. *Mechanical behaviour of the laser-treated materials*

Uniaxial tensile tests were performed on both materials after laser treatment in RD and TD. Fig. 4a gives an overview of the results for

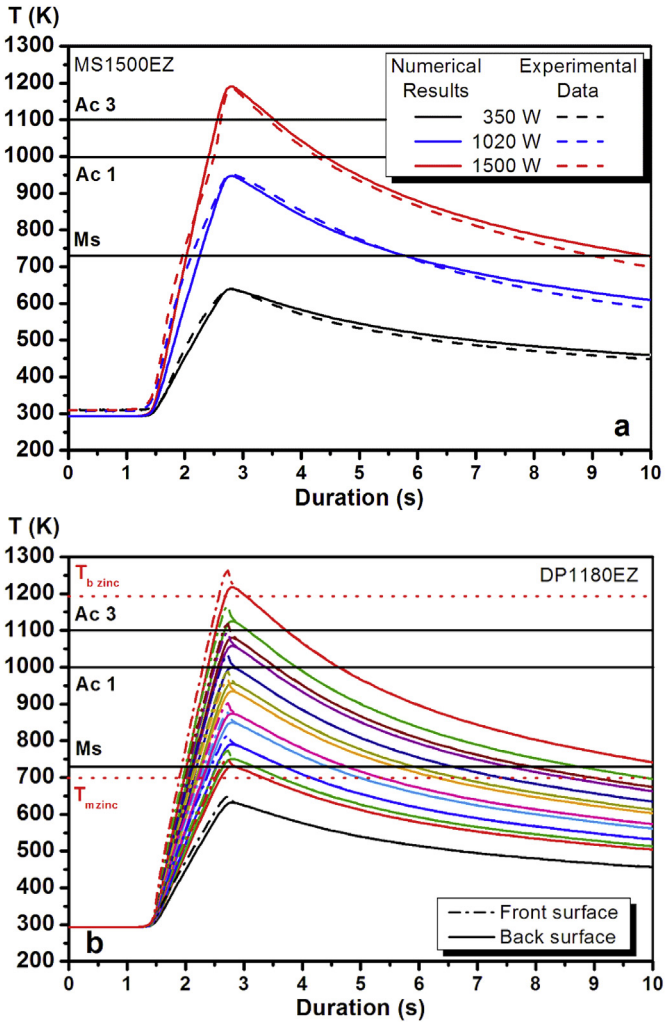

Fig. 3. a) Comparisons between experimental measurements and numerical simulations for MS1500EZ at a scanning rate of 10 mm/s. The coefficient of absorption was taken as 0.57, 0.37, and 0.345 for powers at 350 W, 1020 W, and 1500 W, respectively. b) Modelling of the temperature of a point at the centre of the laser track for each applied condition (320 W − 1300 W) on DP1180EZ.

Table 2
Parameters used in the modelling of laser treatment (based on [25,26]).

λ ($W.m^{-1}.K^{-1}$)	Cp ($J.kg^{-1}.K^{-1}$)	ρ ($kg.m^{-3}$)	α
28	560	7860	Adjusted

DP1180EZ in RD, with only one of the three tested specimens being plotted. The base metal presents a high strength with an ultimate tensile strength (UTS) of around 1200 MPa but a low ductility with almost 5% of uniform plastic deformation (ε_u). As the temperature increased during treatment, the material begins to decrease in strength and gains more ductility up to an optimal treatment.

Fig. 4b and c respectively show the average offset yield stress at 0.2% plastic strain ($\sigma_{0.2\%}$) for the UTS and uniform deformation for both materials in each condition. The two grades of steel behave similarly. Up to 600 K - Ms, very few changes are observed between the base metals and laser-treated samples. Between Ms and Ac1, $\sigma_{0.2\%}$ and UTS decrease linearly with the temperature measured on the back surface. Minimal UTS was reached at Ac1: DP1180EZ had a UTS of 816 +/- 51 MPa in RD and 801 +/- 49 MPa in TD, while MS1500EZ obtained a UTS of 896 +/- 62 MPa in RD and 926 +/- 59 MPa in TD.

Between Ac1 and Ac3, the yield stress kept decreasing. This decrease was more pronounced with temperatures below Ac1. Note that the linear behaviour below Ac1 seems to give the same value of around 550 MPa for both materials if extrapolated to 1150 K. The low number of points between Ac1 and Ac3, especially for MS1500EZ, does not show a relationship between yield stress and temperature reached during treatment. By contrast, UTS increased with temperature between Ac1 and Ac3. For the DP1180EZ samples, this increase is almost symmetrical to the decrease below Ac1.

Above Ac3, yield stress and UTS increased up to constant values. For treatments at the highest power, the RD data match the TD data. UTS reached values of 1510 +/- 105 MPa and 1044 +/- 82 MPa for MS1500EZ and DP1180EZ, respectively. Yield stress remained at a lower level of 1030 +/- 72 MPa and 672 +/- 47 MPa for MS1500EZ and DP1180EZ, respectively.

The materials did not gain in ductility up to 875 K. Above 875 K, the maximum uniform deformation increased rapidly, reaching a peak close to Ac3. At this temperature, the DP1180EZ samples had a uniform elongation of 13.9%+/- 0.5% in RD and 14%+/- 0.45% in TD. This represents an increase by a factor 2.8 compared to the base metal. For MS1500, the data close to Ac3 are missing, although between Ac1 and Ac3 the data correspond to those from DP1180EZ. It is thus very likely that similar values can be reached for MS1500EZ. At 1060 K, the uniform deformation can already reach 8.5% +/- 1.8% in RD and 10.1% +/- 1.8% in TD, which is more than a threefold increase in TD when compared to the base metal.

The strain hardening exponent (n) describes the work hardening capacity of a material and can be defined using the Hollomon analysis [27] with the expression:

$$\sigma = K\varepsilon^n \quad (1)$$

where σ and ε are true tensile stress and strain, respectively.

As typical of steels mainly composed of martensite, the strain hardening exponent of the base metals were found at low values less than 0.1 [28]. The first laser treatments resulted in a slight decrease in the exponent n with temperatures until 860 K. Above this temperature, n increased rapidly. After this initial increase, the value did not seem to change significantly up to Ac3; n stayed at a relatively high level above 0.1, while decreasing as the temperature increased.

To summarise, several temperatures appear to be relevant for laser heat treatment. Ms is a threshold temperature associated with the start of steel softening. Ac1 gives the minimal value of UTS for both materials. Reaching Ac3 results in a minimum of $\sigma_{0.2\%}$ and a maximum of uniform plastic deformation and strain hardening. A fourth threshold

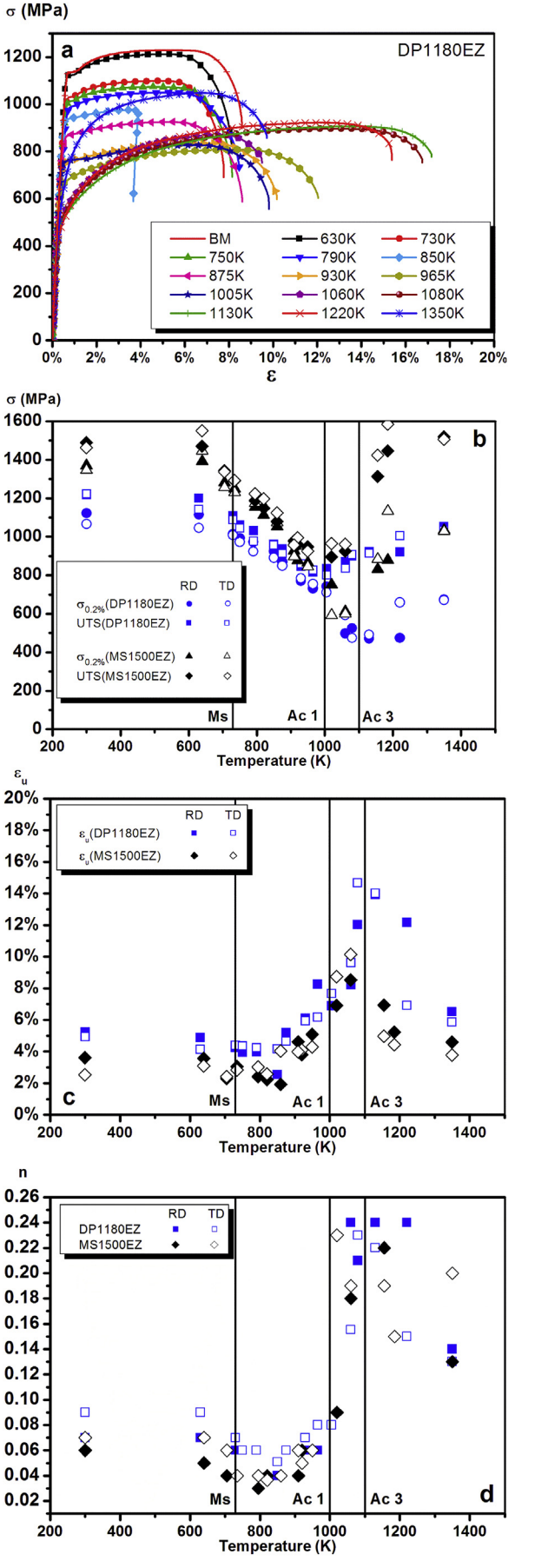

(caption on next page)

Fig. 4. (a) Mechanical behaviour of each laser treatment of DP1180EZ in the rolling direction. Average b) yield stress ($\sigma_{0.2\%}$) and ultimate tensile strength (UTS), c) uniform plastic deformation (ε_u), and d) strain hardening exponent (n) for each laser-treated condition for steels DP1180EZ and MS1500EZ in both the rolling (RD) and transverse directions (TD). The temperature indicated in each graph is the peak temperature measured on the backside of the samples.

temperature around 860–875 K can be added for the increase in ε_u and n.

3.3. Microstructural changes after laser treatment

The SEM observations of the base metals revealed the expected microstructure for both materials. DP1180EZ showed a dual-phase microstructure with a large proportion of martensite, while MS1500EZ was fully martensitic (Fig. 5). The grain size of both materials is in the range of a few tens of micrometres.

Both grades behave similarly during the laser heat treatment. Below Ac1, large spheroidal carbides of a few hundred nanometres appeared in MS1500EZ at 950 K (Fig. 6). The closer to Ac1, the more numerous and larger these carbides are. It is worth noting that these carbides are finer at a similar temperature in DP1180EZ. Above Ac1, new austenite islands are formed during the process despite the short duration at a high temperature. The old grain boundaries are still clearly visible with thin lines on the images.

At Ac3, the microstructure does not seem to have fully transformed to austenite. At 1130 K, a large number of islands appear in DP1180EZ but do not cover the full image (Fig. 7). Moreover, almost no spheroid carbides are left in the microstructure. They may have been dissolved in the matrix or may not have formed at all during treatment.

While treatment above Ac3 leads to a full martensitic microstructure at the highest powers for MS1500EZ, DP1180EZ behaves differently. As seen in Fig. 7 at 1220 K, a ferrite phase remains after laser treatment. The microstructure retains a “dual-phase” structure with a ferrite phase and a second phase mainly composed of martensite with some parts of bainite. This suggests that the applied laser treatment may predominantly influence the initial metastable martensite rather than the ferrite.

3.4. Coating evolution

The electrogalvanised coating was characterised by EDS before and after laser treatment. Three specific parameters were extracted: coating thickness (Fig. 8a) as well as the penetration depth of zinc in the steel and iron in the coating (Fig. 8b). Here, the penetration depth of an element is defined as the distance measured on an EDS profile where the element represents more than 5% of the total chemical elements in the coating or matrix.

Coating thickness did not decrease up to 1180 K, i.e., zinc boiling point. The coating may even become thicker due to a loss of density with the appearance of micrometric pores in the materials. Most treated samples showed a lack of uniformity in the coating. This may be due to the vibration induced by the linear actuator, which allows the sample to be translated under the laser. At high temperatures, these vibrations would lead to the creation of waves in the coating, which is in a liquid state. The rapid cooling would then freeze these waves, thus resulting in large data scattering (Fig. 8a).

Above the zinc boiling point, the coating started to evaporate. No residual coating was observed on the specimens heated above 1250 K.

The diffusion of zinc in the matrix is limited during the process. The presence of zinc is not detected after a few microns, even in the sample corresponding to the highest temperature reached during the tests. By contrast, the quantity of iron in the coating increased with the temperature during treatment, especially when the coating was heated above its melting point. This phenomenon is commonly observed when liquid zinc is deposited on the surface of steel [29]. The presence of iron in zinc generally induces an embrittlement of the zinc coating [29]. On the tensile specimens, this phenomenon leads to the formation of scales on the surface of the samples after the tensile tests.

4. Discussion

4.1. Effect of laser heat treatment

The observed softening of the two grades of steel between Ms and Ac1 correlates well with a tempering of the martensite phase. During conventional tempering treatment at a relatively high temperature, the high carbon content in martensite decreases as carbon atoms diffuse, while coarse particles of cementite appear in the microstructure [30]. With TEM observations, Baltazar et al. [31] compared the isothermal and non-isothermal tempering of dual-phase steels, observing close to 50% of martensite at a subcritical temperature. According to the authors, non-isothermal tempering leads to a finer precipitation of cementite particles of *ca.* 50 nm in size compared to isothermal tempering, for which the particles reached an average size of 230 nm while not allowing a complete recovery of the martensite laths and dislocation network. A drop in hardness of just 10% was observed for non-isothermal tempering compared to a 40% decrease in the case of isothermal treatment. Assuming a linear dependence between hardness and yield stress [32], the decrease would be close to 30% in our study for DP1180EZ, which is three times greater than the authors’ observations. Two reasons may explain the discrepancies between the results reported in Ref. [31] and the present paper. First, DP1180EZ has a higher martensite content than the dual-phase steel used in the study of Baltazar et al., and thus more material can be softened. Second, the heating rate was two to three times higher in their study. It has been noted in the literature that a higher heating rate leads to reduced softening [33] and more refined size distribution of the cementite particles [34].

Above Ac1, the nucleation of austenite grains occurs during laser heat treatment. After nital etching of the material, the matrix appears to be mostly composed of ferrite. Hence, for treatments within the

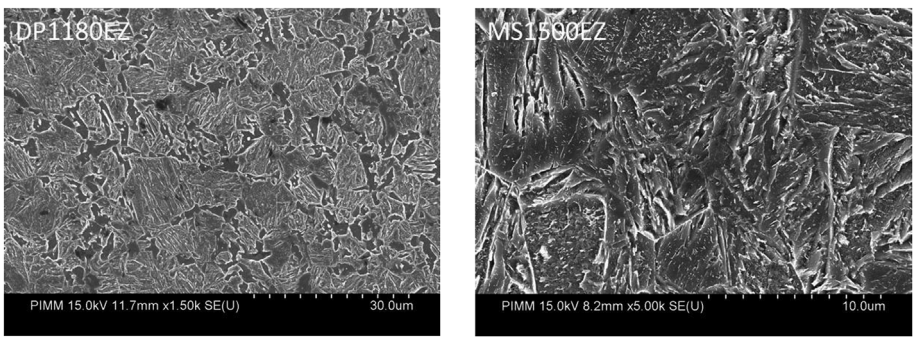

Fig. 5. SEM images of the base metals after nital etching.

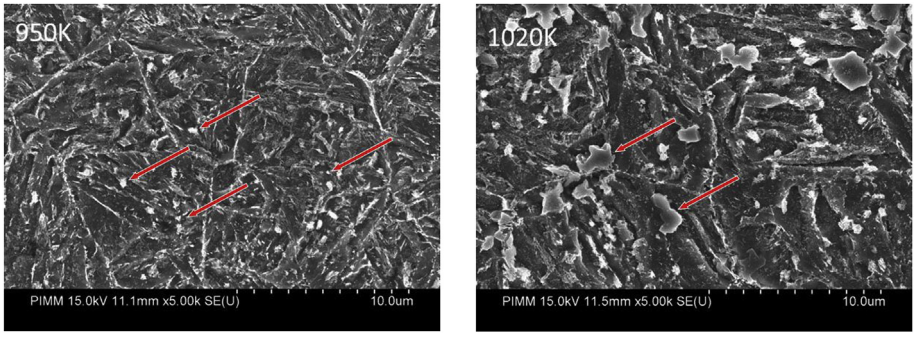

Fig. 6. SEM observations of the microstructural changes in MS1500EZ after laser treatment at 950 K and 1020 K. At 950 K, carbides are observed in the materials, while martensite islands are visible at 1020 K.

intercritical temperature range, the material exhibits a bi-modal distribution of grains, with old grains of ferrite still visible in the SEM along with newly created grains of martensite. This bi-modal distribution with micrometric martensite islands was also obtained by Azizi et al. [35] after flash annealing with a plateau of around 1 s at 1020 K of martensitic steel.

The presence of carbides also seems to be lower in the ferrite matrix above Ac1 compared to below Ac1, which may explain the decrease in yield stress and gain in ductility. Optimal yield stress and uniform deformation lies in the range 1050 K–1150 K, close to Ac3, but it cannot be more accurately determined from the data. From the SEM observations alone, it is difficult to explain why yield stress continues to decrease and uniform plastic deformation to increase as the temperature increases to Ac3 and beyond. Indeed, martensite islands grow with temperature. This coarsening of the hard phase explains why the UTS increases between Ac1 and Ac3, but it does not explicate the observed softening of the material. The explanation may be found at a lower microscopic level, and further investigations of the carbon content in the matrix or the dislocation density may be necessary to explain this behaviour. The strain hardening exponent n after laser treatment is close to the value found on annealed low-carbon steel, which may suggest a good recovery of the dislocation networks and internal stress.

Neugebauer et al. [19] performed multiple laser treatments on dual-phase and martensitic steels between 873 and 1073 K. Although they observe a larger decrease in hardness above 973 K, they do not report a higher drop at 1073 K compared to 973 K. However, a higher content of ferrite phase in the samples heated above 973 K is observed in comparison to the samples treated at lower temperatures.

For treatments above Ac3, the initial martensite phase in the materials seems to completely revert back to an unprocessed phase. The mechanical behaviour of the treated samples tends toward their initial untreated behaviour but with a lower yield stress and slightly enhanced ductility. Moreover, this corroborates well with the SEM observations in which the MS1500EZ samples show a dense martensitic structure at the highest treatment, while the DP1180EZ samples keep a dual-phase structure. The slightly weaker performance of DP1180EZ after high-temperature treatment compared to the base metal may be attributed to the presence of bainite in the second phase instead of a full martensite phase. This restoration to the initial material does not mean that the ferrite phase is unaffected by treatment, but rather that the phase is more stable at higher temperatures than martensite.

Capello et al. [23] compared the behaviour of a dual-phase steel after laser heat treatment with less than 20% of martensite at 875 K (below Ac1) and 1180 K (above Ac3). At 875 K, they found higher yield stress and ductility as well as lower UTS, which is consistent with our findings, except for ductility, which was higher at 1180 K in our study. Contrary to the present results, they observed a massive change in the microstructure after treatment at 1180 K, with a complex mixture of tempered martensite, bainite, and ferrite. The cooling rate of their treatment was two to four times slower than ours due to their choice of a lower scanning rate. Indeed, a fast cooling rate may limit the formation of bainite [36], which is in agreement with previous studies showing the absence or low amounts of bainite after the welding of dual-phase [37,38] or martensitic steels [39].

4.2. *Laser treatment process on galvanised AHSS*

Laser treatments were performed on commercially available galvanised grades of AHSS. The manufacturer used galvanisation to promote the resistance to corrosion. Although the zinc coating was not found to negatively influence the treatments of the underneath steel, its evolution during the process significantly deteriorated its anticorrosion properties. In particular, its lack of uniformity and embrittlement after treatment do not meet industrial standards. Hence, from an industrial point of view, the galvanisation process should be performed after any laser heat treatment of the sheets.

The laser heat treatment applied to high martensite content steels locally and significantly reduces the yield stress and multiplies the uniform plastic elongation by a factor 3. This makes the process appealing for a number of industrial material forming applications. One

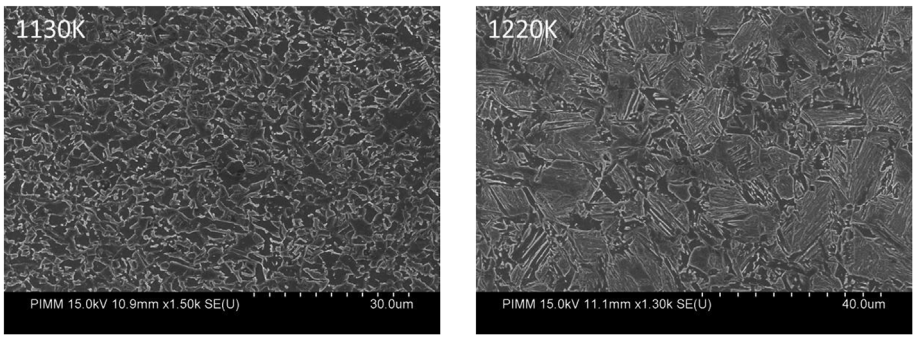

Fig. 7. Comparison between two laser treatments close to Ac3 and 200 K above Ac3 on DP1180EZ.

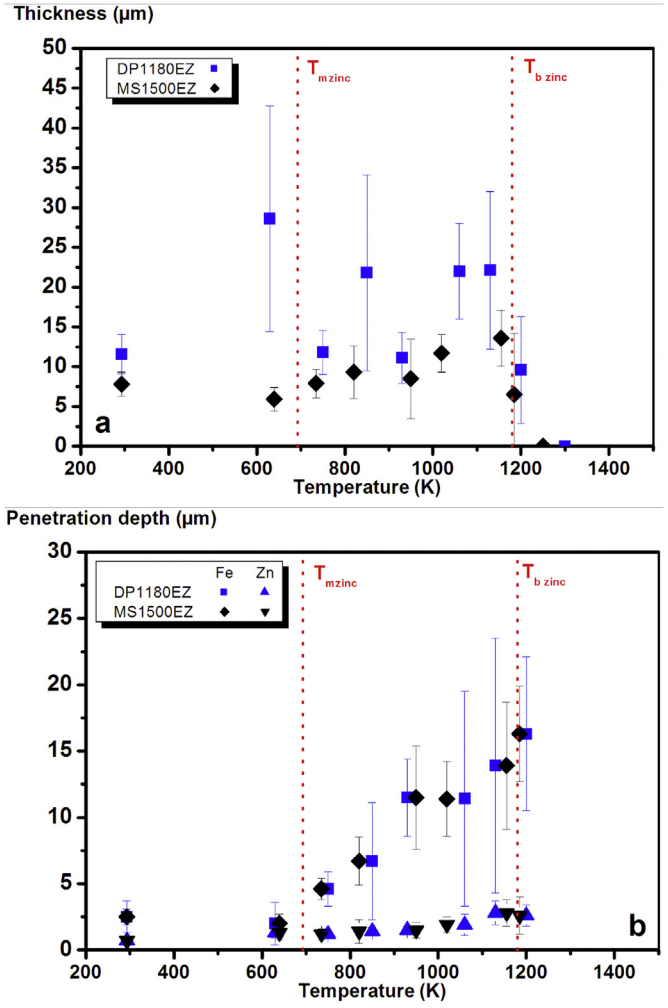

Fig. 8. a) Coating thickness and b) diffusion of zinc in the matrix and iron in the coating after laser treatment at a given temperature.

example is cold stamping. This forming process is limited by two parameters: stretchability [40] and spring back effect [41]. The stretchability of a sheet can be related to the ductility of the material, since, by definition, more ductile material can accommodate more deformation. The spring back phenomenon can be defined as the additional elastic deformation of a structural component after the removal of forming loads. This effect is controlled by the yield stress of the material, as the additional deformation results from the elastic relaxation of the part. Hence, laser treatment at temperatures just below Ac3 greatly improves the stamping formability of a piece, as it increases the stretchability of the sheet and reduces the spring back effect. Moreover, the untreated part of the component retains its high mechanical properties for any structural purpose.

The tensile specimens were sampled on a small area compared to the laser spot. The mechanical properties of the material were thus close to uniform on the specimen. However, this is not the case for a manufactured component without milling out the treated area. For laser treatment at Ac3, the thermal gradient means that an area on the surface of the sheet will only be heated at Ac1. This area will have a low UTS according to our data. Furthermore, if the temperature on the backside reaches a value superior to Ac1, then the temperature will only reach Ac1 on a continuous area throughout the entire sheet from the front to the back surface. This weak spot should thus be further considered for any structural load.

Temperature uniformity of the sheet is determined by the ratio between the spot size of the laser and the thickness of the sheet (t). The

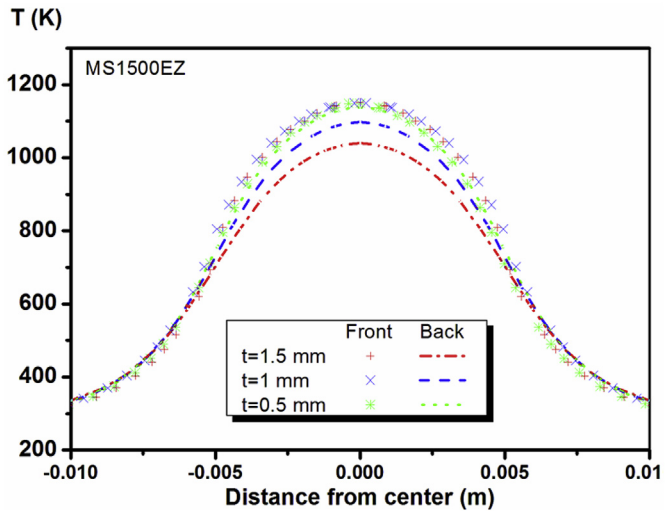

Fig. 9. Spatial distribution of temperature on the irradiated front and back surface of sheets with different thicknesses. The temperature was modelled for a square laser spot of 1 cm^2 and scanning rate of 10 mm/s.

higher the ratio, the more uniform the temperature is through the sample for the same temperature reached on surface (Fig. 9). For a square laser spot of 1 cm^2 and a scanning rate of 10 mm/s, the temperature difference is about 50 K between the irradiated front and back surface of a 1-mm-thick steel sheet, while it reaches 110 K for 1.5-mm thickness and only 10 K for 0.5-mm thickness. Hence, depending on the level of precision regarding the temperature and dimension of the treated area, the spot size should be optimised. A larger spot should be preferred to ensure the uniformity of heat treatment and a small spot to accurately treat specific areas.

5. Conclusions

The changes in mechanical behaviour of martensitic and dual-phase steel after laser treatment were extensively studied over a large range of temperatures and supplemented with microstructural characterisations. Several points of interest were identified.

First, laser heat treatment at temperature Ac1 leads to the most severe reduction in UTS for MS1500EZ and DP1180EZ. Second, intercritical heat treatment close to Ac3 leads to maximum ductility and minimum yield stress. The uniform plastic deformation is multiplied by at least a factor 3 and yield stress by a factor 2 for optimal treatment. Third, the microstructures for both materials change from a tempering of the martensite phase for a treatment below Ac1 to a dual-phase structure between Ac1 and Ac3. After treatment above Ac3, a full martensitic structure is observed in MS1500EZ, while a “dual-phase” microstructure of martensite/bainite and ferrite is seen in DP1180EZ. Finally, the zinc coating does not behave well during high-temperature treatments. Galvanisation after the laser process would thus be preferable.

Acknowledgements

This study was funded by Agence Nationale de la Recherche through the ANR JCJC SCOLASTIC project (grant no. 16-CE08-0009). The support of AcerlorMittal R&D in supplying the material used in this study is also gratefully acknowledged.

References

[1] W. Miller, et al., Recent development in aluminium alloys for the automotive industry, Mater. Sci. Eng., A 280 (1) (Mar. 2000) 37–49.
[2] K.-M. Hong, Y.C. Shin, Prospects of laser welding technology in the automotive

industry: a review, J. Mater. Process. Technol. 245 (Jul. 2017) 46–69.
[3] R. Kuziak, R. Kawalla, S. Waengler, Advanced high strength steels for automotive industry, Arch. Civ. Mech. Eng. 8 (2) (Jan. 2008) 103–117.
[4] M. Shome, M. Tumuluru (Eds.), Welding and Joining of Advanced High Strength Steels (AHSS), Woodhead, Cambridge, 2015.
[5] O. Bouaziz, H. Zurob, M. Huang, Driving force and logic of development of advanced high strength steels for automotive applications, Steel Res. Int. 84 (10) (Jun. 2013) 937–947.
[6] Q. Lai, et al., Influence of martensite volume fraction and hardness on the plastic behavior of dual-phase steels: experiments and micromechanical modeling, Int. J. Plast. 80 (May 2016) 187–203.
[7] V.S. D'yachenko, G.N. Tverdokhlebov, A.A. Korosteleva, Features of laser heat treatment of high-speed steel tools, Met. Sci. Heat Treat. 26 (9) (Sep. 1984) 675–679.
[8] A. Jahn, M. Heitmanek, J. Standfuss, B. Brenner, G. Wunderlich, B. Donat, Local laser strengthening of steel sheets for load adapted component design in car body structures, Phys. Procedia 12 (2011) 431–441.
[9] I. Watanabe, M. McBride, P. Newton, K.S. Kurtz, Laser surface treatment to improve mechanical properties of cast titanium, Dent. Mater. 25 (5) (May 2009) 629–633.
[10] D.-G. Shang, C.-G. Ren, H. Liu, L. Wang, Approach to recovery of fatigue damage for copper film by pulsed laser irradiation, Surf. Eng. 29 (7) (Aug. 2013) 536–542.
[11] Y. Chi, G. Gu, H. Yu, C. Chen, Laser surface alloying on aluminum and its alloys: a review, Optic Laser. Eng. 100 (Jan. 2018) 23–37.
[12] M.F. Ashby, K.E. Easterling, "The transformation hardening of steel surfaces by laser beams—I. Hypo-eutectoid steels, Acta Metall. 32 (11) (Nov. 1984) 1935–1948.
[13] K. Bandyopadhyay, S.K. Panda, P. Saha, Investigations into the influence of weld zone on formability of fiber laser-welded advanced high strength steel, J. Mater. Eng. Perform. 23 (4) (Apr. 2014) 1465–1479.
[14] M. Xia, N. Sreenivasan, S. Lawson, Y. Zhou, Z. Tian, A comparative study of formability of diode laser welds in DP980 and HSLA steels, J. Eng. Mater. Technol. 129 (3) (2007) 446.
[15] G. Krauss, Martensite in steel: strength and structure, Mater. Sci. Eng., A 273–275 (Dec. 1999) 40–57.
[16] W. Yan, L. Zhu, W. Sha, Y. Shan, K. Yang, Change of tensile behavior of a high-strength low-alloy steel with tempering temperature, Mater. Sci. Eng., A 517 (1–2) (Aug. 2009) 369–374.
[17] A. Saastamoinen, A. Kaijalainen, J. Heikkala, D. Porter, P. Suikkanen, The effect of tempering temperature on microstructure, mechanical properties and bendability of direct-quenched low-alloy strip steel, Mater. Sci. Eng., A 730 (Jul. 2018) 284–294.
[18] A. Weisheit, G. Vitr, K. Wissenbach, J. Zajac, H. Thoors, B. Johansson, E. Ribera, J. Ariño, F. Sierra, Local Heat Treatment of Ultra High Strength Steels to Improve Formability, IWOTE, 2005, pp. 63–81.
[19] R. Neugebauer, S. Scheffler, R. Poprawe, A. Weisheit, Local laser heat treatment of ultra high strength steels to improve formability, Prod. Eng. 3 (4–5) (Dec. 2009) 347–351.
[20] S. Vogt, L. Bechheim, J. Banik, M. Flaischerowitz, A. Weisheit, J.H. Schleifenbaum, Local laser softening of press-hardened steel at high feed rates, J. Laser Appl. 30 (3) (Aug. 2018) p. 031201.
[21] B.V.H. Hernandez, M.L. Kuntz, M.I. Khan, Y. Zhou, Influence of microstructure and weld size on the mechanical behaviour of dissimilar AHSS resistance spot welds, Sci. Technol. Weld. Join. 13 (8) (Nov. 2008) 769–776.
[22] N. Sreenivasan, M. Xia, S. Lawson, Y. Zhou, Effect of laser welding on formability of DP980 steel, J. Eng. Mater. Technol. 130 (4) (2008) p. 041004.
[23] E. Capello, B. Previtali, Enhancing dual phase steel formability by diode laser heat treatment, J. Laser Appl. 21 (1) (Feb. 2009) 1–9.
[24] K.W. Andrews, Empirical formulae for the calculation of some transformation temperatures, J. Iron Steel Inst. 203 (1965) 721–727.
[25] H.G. Woo, H.S. Cho, Three-dimensional temperature distribution in laser surface hardening processes, Proc. Inst. Mech. Eng. Part B J. Eng. Manuf. 213 (7) (Jul. 1999) 695–712.
[26] H. Pantsar, V. Kujanpää, Effect of oxide layer growth on diode laser beam transformation hardening of steels, Surf. Coating. Technol. 200 (8) (Jan. 2006) 2627–2633.
[27] J.H. Hollomon, Trans. Metall. Soc. AIME 162 (1945) 268–290.
[28] M. Umemoto, K. Tsuchiya, Z.G. Liu, S. Sugimoto, Tensile stress-strain analysis of single-structure steels, Metall. Mater. Trans. 31 (7) (Jul. 2000) 1785–1794.
[29] A.R. Marder, The metallurgy of zinc-coated steel, Prog. Mater. Sci. 45 (3) (Jun. 2000) 191–271.
[30] G. Krauss, Tempering of lath martensite in low and medium carbon steels: assessment and challenges, Steel Res. Int. 88 (10) (Oct. 2017) p. 1700038.
[31] V.H. Baltazar Hernandez, S.S. Nayak, Y. Zhou, Tempering of martensite in dual-phase steels and its effects on softening behavior, Metall. Mater. Trans. 42 (10) (Oct. 2011) 3115–3129.
[32] J.T. Busby, M.C. Hash, G.S. Was, The relationship between hardness and yield stress in irradiated austenitic and ferritic steels, J. Nucl. Mater. 336 (2–3) (Feb. 2005) 267–278.
[33] M. Xia, E. Biro, Z. Tian, Y.N. Zhou, Effects of heat input and martensite on HAZ softening in laser welding of dual phase steels, ISIJ Int. 48 (6) (2008) 809–814.
[34] A. Nagao, K. Hayashi, K. Oi, S. Mitao, N. Shikanai, Refinement of cementite in high strength steel plates by rapid heating and tempering, Mater. Sci. Forum 539 (543) (Mar. 2007) 4720–4725.
[35] H. Azizi-Alizamini, M. Militzer, W.J. Poole, A novel technique for developing bimodal grain size distributions in low carbon steels, Scripta Mater. 57 (12) (Dec. 2007) 1065–1068.
[36] W. Xu, D. Westerbaan, S.S. Nayak, D.L. Chen, F. Goodwin, Y. Zhou, Tensile and fatigue properties of fiber laser welded high strength low alloy and DP980 dual-phase steel joints, Mater. Des. 43 (Jan. 2013) 373–383.
[37] D. Dong, Y. Liu, Y. Yang, J. Li, M. Ma, T. Jiang, Microstructure and dynamic tensile behavior of DP600 dual phase steel joint by laser welding, Mater. Sci. Eng., A 594 (Jan. 2014) 17–25.
[38] N. Farabi, D.L. Chen, Y. Zhou, Tensile properties and work hardening behavior of laser-welded dual-phase steel joints, J. Mater. Eng. Perform. 21 (2) (Feb. 2012) 222–230.
[39] D. Shirmohammadi, M. Movahedi, M. Pouranvari, Resistance spot welding of martensitic stainless steel: effect of initial base metal microstructure on weld microstructure and mechanical performance, Mater. Sci. Eng., A 703 (Aug. 2017) 154–161.
[40] Y. Tokita, T. Nakagaito, Y. Tamai, T. Urabe, Stretch formability of high strength steel sheets in warm forming, J. Mater. Process. Technol. 246 (Aug. 2017) 77–84.
[41] M.R. Stoudt, L.E. Levine, L. Ma, Designing a uniaxial tension/compression test for springback analysis in high-strength steel sheets, Exp. Mech. 57 (1) (Jan. 2017) 155–163.